Arab J Sci Eng (2015) 40:2503–2514
DOI 10.1007/s13369-015-1658-1

RESEARCH ARTICLE - COMPUTER ENGINEERING AND COMPUTER SCIENCE

Real-Time ECG Noise Reduction with QRS Complex Detection for Mobile Health Services

Chakchai So-In[1] · **Comdet Phaudphut**[1] · **Kanokmon Rujirakul**[1]

Received: 21 August 2014 / Accepted: 13 April 2015 / Published online: 4 May 2015

Abstract Cardiovascular disease is a serious threat to human life, especially when a sudden attack occurs, so real-time patient monitoring is crucial. Recent advances in health care and technology have led to equipment such as mobile micro-electro-mechanical systems, which can be used for more accessible public healthcare services. Electrocardiogram (ECG) data are traditionally used to investigate and monitor heart activities. However, the necessary electronic logic tags and (wireless) signal transmissions in a mobile healthcare device are susceptible to noise, which can result in false interpretations. Consequently, this study proposed a novel, low-complexity method for generating an optimized ECG wave suitable for mobile architecture. We first apply a bi-quad, high-pass filter to adjust baseline drifts. Then, a Savitzky–Golay filter smoothes the raw ECG, and moving variance and integral filters with thresholds are used to determine the QRS complex. We compared the results of the proposed technique to those from the moving average, Savitzky–Golay, PRASMMA, and Pan–Tompkins algorithms, using the well-known QT and MIT-BIH databases, and human subjects. The method was implemented on a mobile device integrating an open ECG platform as a prototype for real-time ECG monitoring systems.

✉ Chakchai So-In
chakso@kku.ac.th

Comdet Phaudphut
comdet@kkumail.com

Kanokmon Rujirakul
kanokmon.r@glive.kku.ac.th

[1] Applied Network Technology (ANT) Laboratory, Department of Computer Science, Faculty of Science, Khon Kaen University, Khon Kaen, Thailand

Keywords Cardiovascular · Electrocardiogram · Mobile health service · Noise reduction · QRS complex detection · Smoothing filter

1 Introduction

Approximately 17 million people suffer from cardiovascular disease every year. This includes heart attack and stroke patients, but excludes patients requiring periodic treatments [1]. Most severe cases (including those that result in death) are due to a sudden attack, where the patient did not receive aid on time.

Recent advances in computing and electronic devices have been integrated into healthcare environments and play an important role in real-time health monitoring, prevention, and treatment [2,3]. In particular, micro-electro-mechanical systems have resulted in accessible and affordable medical equipment that performs well and is portable. Examples of such equipment include body sensors [4].

Advances in mobile networking technologies have led to an increase in mobile (smart) phones at ever-shrinking costs. These technologies can provide more functionality, including open systems such as Android [5]. This means that mobile phones can be integrated with healthcare sensors [6–9].

Electrocardiogram (ECG) signals generated from the human heart are frequently used for investigations and monitoring. They can be used to monitor abnormal heart functions [10–12]. Several medical and research companies have focused on improving sensing equipment such as ECG sensor tags and ECG recognition processors [13–15].

Although the sensing capabilities of ECG sensor tags and acquisition models have improved, electronic, thermal, and transmission noises can be introduced when the data are transmitted wirelessly (e.g. from a portable device). Like-

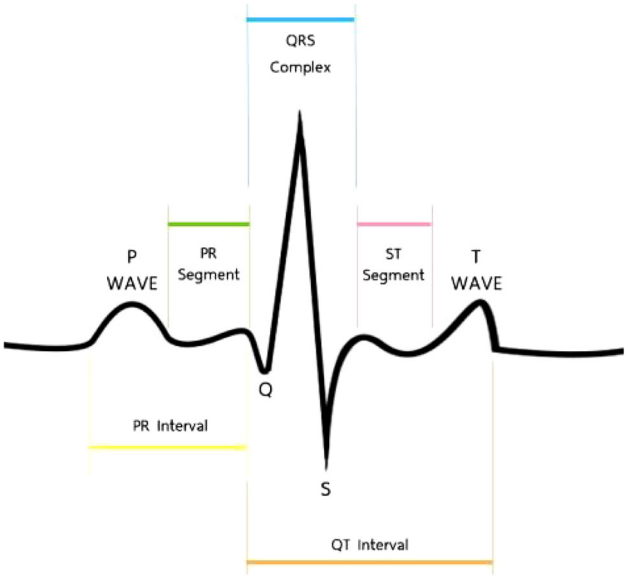

Fig. 1 Example of an ECG waveform (*Q*, *R*, *S*, and *T* waves)

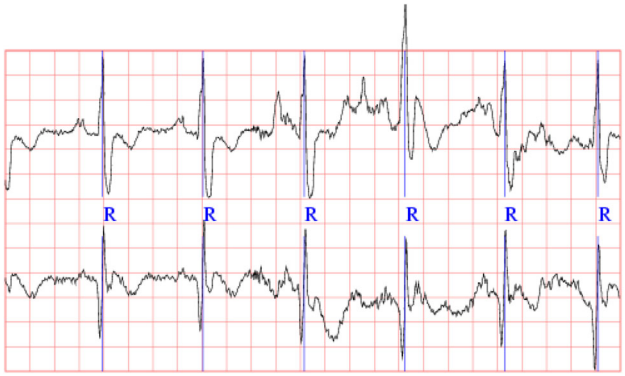

Fig. 2 Example of muscle and motion noise [24]

wise, the waveform can be affected by human behaviours and activities that can electrically interfere with the ECG. These issues may lead to medical misinterpretations.

Electrocardiogram waves are generally represented by their QRS complex. This is the name for the three graphical deflections (excluding the *P* and *T* waves) that are the most visually obvious portions of the heartbeat. The QRS complex corresponds to the depolarization of the right and left ventricles of the heart. An example ECG waveform is shown in Fig. 1. Typically, there are five deflections in an ECG, referred to as waves *P* to *T*. The *Q*, *R*, and *S* waves occur in rapid succession. The *Q* wave is a downward deflection after a *P* wave. Next, the *R* wave is an upward deflection, and the *S* wave follows as a downward deflection. The *T* wave follows the *S* wave [11,13,16].

ECG-based systems have several components including design optimization [17,18], ECG pre-processing [19], and ECG analysis and classification [12,13,20]. However, we focused on two issues: detecting the ECG QRS complex and reducing the noise in real-time applications.

To achieve these goals, we considered three facets: (1) improving the noise reduction techniques, i.e. using a Savitzky–Golay filter [21,22] instead of the traditional moving average [23]; (2) detecting the QRS complex period for medical diagnoses using the moving variance and integral with thresholds; and (3) a low-complexity implementation on mobile ECG platforms, i.e. Android OS.

The remainder of this paper is organized as follows. In Sect. 2, we present an overview of ECG noise types. We provide a brief survey of recent proposals regarding QRS complex detection with noise reduction in Sect. 3. In Sect. 4, we present our low-complexity, real-time noise reduction method for detecting QRS complexes. Then, we discuss the detailed mobile architecture implementation in Sect. 5 and the performance of our method in Sect. 6. Finally, our conclusions and suggestions for future work are given in Sect. 7.

2 Overview of ECG Noise Types

To conduct a non-invasive ECG recording, several electrodes are attached to different parts of the body. The recording is typically exposed to various noises or artefacts, depending on the frequency ranges. The noise can be divided into two classes: persistent and burst [19].

Persistent noise is correlated with the signals coming from the electrodes and has a similar temporal distribution but different intensity levels. These noises reside in a variety of frequency bands (low-frequency, medium-frequency, and high-frequency signals [26]). In this research, we considered three types of noise by selecting intervals that contained predominantly baseline wander, muscle artefacts, and electrode motion artefacts [24,27]. Examples of these noise types are shown in Fig. 2.

Power-line noise is another type of persistent noise. It typically originates from utility company equipment and is caused by sparking or arcing across power-line-related hardware or by alternating currents between 50 and 60 Hz [25]. An example of power-line noise is shown in Fig. 3. Power lines can generate undesirable signals that sometimes override or compete with radio signals and can potentially directly impact mobile ECG communications.

Burst noise is white Gaussian noise (WGN) that appears on a subset of electrodes for a very short duration. This type includes electrode pop noise, electrode motion artefacts, or electro-surgical noise [28]. The frequency of this type of noise is generally not well defined, although an example is shown in Fig. 4 [19].

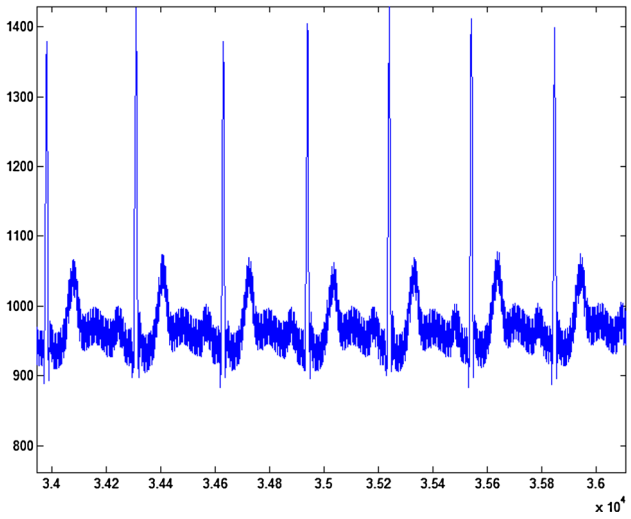

Fig. 3 Example of power-line noise [25]

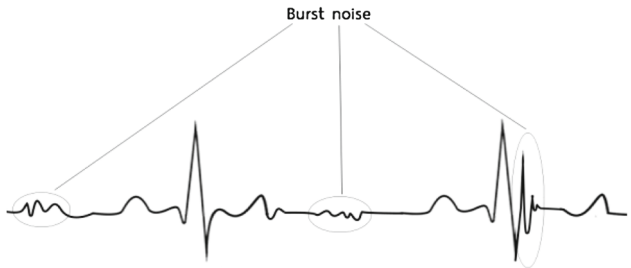

Fig. 4 Example of burst noise [19]

3 Related Work

Several different approaches have been proposed to mitigate the effects of noise and improve the QRS complex. The aim of these methods is to identifying the individual terms of the ECG signals, i.e. Q, R, S, T, and P. For example, Pan and Tompkins [29] proposed a QRS complex detection method called the Pan–Tompkins algorithm. The algorithm includes a pre-processing step and can be divided into six main steps: band-pass filter (low- and high-pass), derivation, squaring function, moving window integration, fiducial mark, and thresholds. It is used as a standard for other QRS complex detection methods.

In 2010, Zeraatkar et al. [30] proposed a hybrid technique for QRS complex detection to reduce artefacts from various sources. They incorporated baseline drift removal and notch filtering techniques. Akshay et al. [17] applied an undecimated wavelet transform to remove ECG noise, resulting in a higher accuracy than traditional discrete wavelet transform methods. Lina and Xinhua [31] used a compressed wavelet variant coefficient with wavelet threshold de-noising.

In 2012, Lewandowski et al. [32] introduced a robust, real-time, QRS complex detection method for noisy applications. They used the modified curve length with adaptive threshold derived from the mean, standard deviation, and average peak-to-peak intervals.

Similarly, Changmok et al. [33] implemented a QRS complex detection algorithm for wearable ECG equipment, using proportional derivative control to eliminate small fluctuations of the QRS complex and avoid falsely detecting noise. Additionally, Arafat et al. [34] applied a smoothing ECG signal technique with a Gaussian function waveform to eliminate signal wrinkles and smooth ECG waves.

Recently, Perlman et al. [35] proposed an algorithm for enhancing foetal ECG signals using a modified linear combination algorithm.

Although several methods have been proposed, most approaches lack implementation details, are not appropriate for mobile computing, and/or do not consider the effects of noise on the accuracy of the QRS complex. Additionally, previous publications have not investigated the complexities of the algorithms so that they can be used practically.

Advances in mobile networking technologies have led to increased portability and universal access to real-time communications. Some researchers have considered integrating these technologies into ECG monitoring techniques. For example, Gradl et al. [36] developed a mobile application for monitoring ECG waves in real-time, using SHIMMER sensors as a prototype. Chan et al. [37] also proposed a diagnostic model for mobile ECG monitoring combining mobile phone and cloud services.

Recently, So-In et al. [8] developed architecture for mobile ECG recognition systems using a mobile phone integrated with external ECG sensors. They also proposed back-end systems for further analysis that used a hybrid wavelet transform to extract features. However, most of these developments do not address noise reduction for wirelessly transmitted ECG data.

4 Real-time ECG Noise Reduction for QRS Complex Detection Systems

A measured ECG signal, particularly one that is transmitted wirelessly, can be skewed or fluctuate because of various noises. So we must reduce the noise in ECG signals to make accurate interpretations.

To illustrate the proposed method, Fig. 5 shows an actual ECG wave that is contaminated by noise (blue line). To aid the medical diagnosis, moving average techniques are typically applied to generate a readable waveform. Figure 5 also shows the result of applying a simple moving average (red line). In this research, we applied the Savitzky–Golay filter [21,22] (green line), which results in a waveform that is close to the raw ECG.

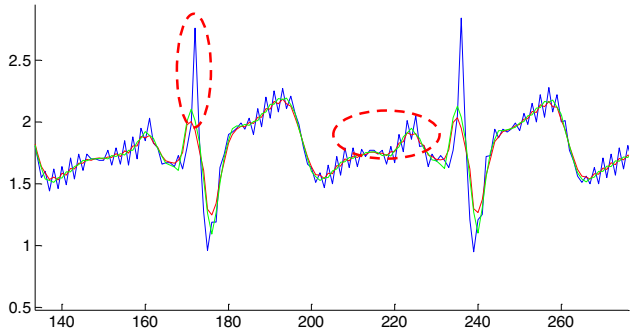

Fig. 5 ECG waveform with smoothing

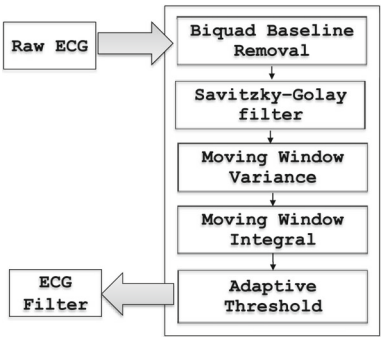

Fig. 6 Proposed noise reduction method

However, this smoothing technique can eliminate QRS complex information, especially the R-peak. This can then lead to a misinterpretation during the medical analysis. The peak rejection adaptive sampling modified moving average (PRASMMA) [23] is a promising technique for dealing with this issue. First, it estimates the inter-beat (RR) interval within a given window. Next, the local maximum is determined to estimate the R-peak based on three sections (before, during, and after the QRS complex). However, PRASMMA has a limited accuracy. It estimates the subsequent ECG beat using five RR intervals. This means that it can misinterpret the beat if it does not have a consistent rate.

Thus, we also propose a method for deriving a readable ECG signal in the presence of various noise types. The proposed method is illustrated in Fig. 6 and is called real-time ECG noise reduction with a QRS complex detection system (RT-ECG). It consists of five main submethods: high-pass baseline drift removal, Savitzky–Golay filter smoothing, moving window variance, moving window integral, and adaptive threshold decision.

Note that the traditional Pan–Tompkins method has six main stages. Additionally, it does not include noise reduction procedures to avoid extra-computational complexity. To achieve a low-complexity detection system that combines the smoothing factor with the RT-ECG, we have combined the second and third stages into a moving variance parameterized for a moving window stage. We added the Savitzky–Golay filter to smooth the noise, but only used a modified adaptive threshold. These combinations result in an algorithm complexity of $O(5n)$.

- *High-pass baseline drift removal*. To support real-time processing, we first apply a high-pass, bi-quad filter [38] to remove the baseline drift from the ECG waveform. We selected a cut-off frequency of 0.5 Hz for noise removal purposes [39]. In the following equations, x_n is the input, y_n is the output, f_s is the sample frequency, and Q is the cut-off frequency.

$$\begin{aligned} y_n &= a_1 x_n + a_2 x_{n-1} + a_3 x_{n-2} - b_1 y_{n-1} - b_2 y_{n-2}. \\ K &= \tan(f_s \pi) \\ a_1 &= \frac{1}{1 + \frac{K}{Q} + K^2} \\ a_2 &= -2 \times a_1 \\ a_3 &= a_1 \\ b_1 &= 2a_1(K^2 - 1) \\ b_2 &= a_1 \left(1 - \frac{K}{Q} + K^2\right) \end{aligned} \tag{1}$$

- *Savitzky–Golay filter smoothing*. We used the Savitzky–Golay smoothing filter. Equation (2) shows the smoothing derivative for sample i in convolution form (S). That is,

$$\begin{aligned} S(i) = &\sum_{k=-\frac{m-1}{2}}^{k=\frac{m-1}{2}} C_k \mathrm{ECG}_{i+k} | \frac{m+1}{2} \le i \\ &\le n - \frac{m-1}{2}. \end{aligned} \tag{2}$$

  Here, ECG is the signal in the time domain, C is a coefficient, m is a quadratic polynomial constant, and n is the sample size.
- *Moving window variance*. We calculated a variance (V) over the window size (w) of sample i derived from the Savitzky–Golay filter, as a key feature to determine the QRS complex boundary. That is,

$$\bar{S} = \sum_{j=0}^{w-1} S(i-j)/w, \tag{3}$$

$$V(i) = \sum (S(i) - \bar{S})^2 / w. \tag{4}$$

- *Moving window integral*. Given a variance, we applied a moving window (M), a multiple of 0.06 by the sampling rate, as a post-processing step to retrieve integral factor (K). That is,

$$\begin{aligned} K(i) = \frac{1}{M} &[V(i - (M-1)) \\ &+ V(i - (M-2)) + \cdots + V(i)]. \end{aligned} \tag{5}$$

- *Adaptive threshold decision*. To ultimately determine the QRS complex, we applied an adaptive threshold (T) over the integral factor as follows.

$$Y(i) = \begin{cases} S(i), K(i) < T(i) \\ \text{ECG}(i), K(i) \geq T(i) \end{cases} \quad (6)$$

$$A(0) = \text{MAX}\{K(j) \times C1\}, j = \{1, \ldots, \text{WS}\}, \quad (7)$$

$$A(i) = \text{MAX}\{K(i-j) \times C1\}, j = \{0, \ldots, \text{WS}\},$$

$$T(1) = A(0), \quad (8)$$

$$T(i) = \begin{cases} T(i-1) + (|A(i) - A(i-1)| \times C2) \\ \quad |A(i) > A(i-1) \\ T(i-1) - (|A(i) - A(i-1)| \times C2) \\ \quad |A(i) < A(i-1) \\ T(i-1) \\ \quad |A(i) = A(i-1). \end{cases}$$

Here, $C1$ is derived from the relationship between the noise and maximum value of the variance (0.04 in this case). $C2$ is a constant derived from the training sampling frequency (e.g. 0.05). *WS* denotes a predefined window sampling size.

Figure 7 shows an example ECG waveform transformation for each step, i.e. from baseline removal to applying the smoothing and filter techniques. This figure illustrates the noise reduction and QRS complex preservation methods. Note that the proposed method achieves three goals. First, it presents real-time detection with a limited number of samples. Second, it preserves the principal component of the QRS complex. Finally, it is highly accurate with a low complexity.

5 Mobile System Architecture

The proposed method has six main modules when implemented on an Android mobile phone [5], as shown in Fig. 8.

- *Bluetooth thread*: This module receives the signal from the ECG sensor tag and stores the raw ECG data into a buffer based on a standard Bluetooth Android OS API [40]. The data are then sent to the second module for fast signal transmission to mitigate packet losses.
- *Device control protocol (DCP) thread*: With a streaming ECG packet, this module is used to disaggregate the control signals from the data signal. In other words, the raw ECG data are extracted into a suitable waveform format for further interpretation, along with the control data.
- *ECG noise reduction thread*: This is a key module that reduces the ECG noise. It applies QRS complex detection functions to the raw ECG data from the DCP.
- *GUI controller thread*: After eliminating the noise, this module interacts with the patient using external communications such as sounds or a display on the Android OS mobile device. In the prototype, we used a canvas library [40] to plot the ECG wave on a mobile phone screen.
- *GPS and map processing thread*: This module functions as a tracking and tracing device, recording a global position (GPS if outdoors, or an embedded location from service providers if indoors).
  This information is used to display the current location of the patient (using the built-in GPS on Android OS phones) on a map (e.g. Google Maps). It notifies other parties (e.g. an emergency unit) of the patient's current location so that help can be sent if necessary.
- *Network streaming controller thread*: This component is the main interaction module (data transmitter) between each component. Note that direct communication between mobile devices is another possible solution [8,9].

The focus of this research was not the ECG sensor tag and its transmission. However, as a practical prototype, these components are generally based on *e-health* sensors using an ATmega328 Arduino (16 MHz) board [41] optimized for integration with mobile phone architectures. Figure 9 shows a schematic of the controller. The platform is an embedded INA321EA amplifier with a 10-bit ADC [41]. The ECG sampling frequency was 250 Hz (±2 ms data latency and Bluetooth class 2 transmission for 4 dBm power). Figure 10 shows an actual prototype of an ECG sensor tag and ECG controller.

Figures 11 and 12 show an actual ECG signal illustration on the screen of a Samsung Galaxy Nexus [5], before and after applying the noise reduction technique.

Algorithm 1 shows the noise reduction algorithm for detecting the QRS complex, starting with the current sample reading from the Bluetooth buffer for the predefined sampling and cut-off frequencies (f_s and Q). Next, we apply the baseline removal process using a bi-quad filter (Line 1), which causes a delay before computing the convolution form of the sample using the Savitzky–Golay method (Lines 2–4).

Then, we calculate the variance and integral factors (Lines 5–13) before obtaining the threshold for making a final decision (Lines 14–21) and retrieving a shaped signal (Lines 22–24). Here, $m = 15$, $w = 15$, $M = 20$, and $f_s = 250$. The complexity of the algorithm was $O(5n)$. To support real-time computation, the actual implementation was written in native C to produce a fast analysis (less than 1 ms per sample). As shown in the algorithm, only 33 samples were required.

6 Performance Evaluation

In this section, we present the results of our evaluation to show that the method performs well.

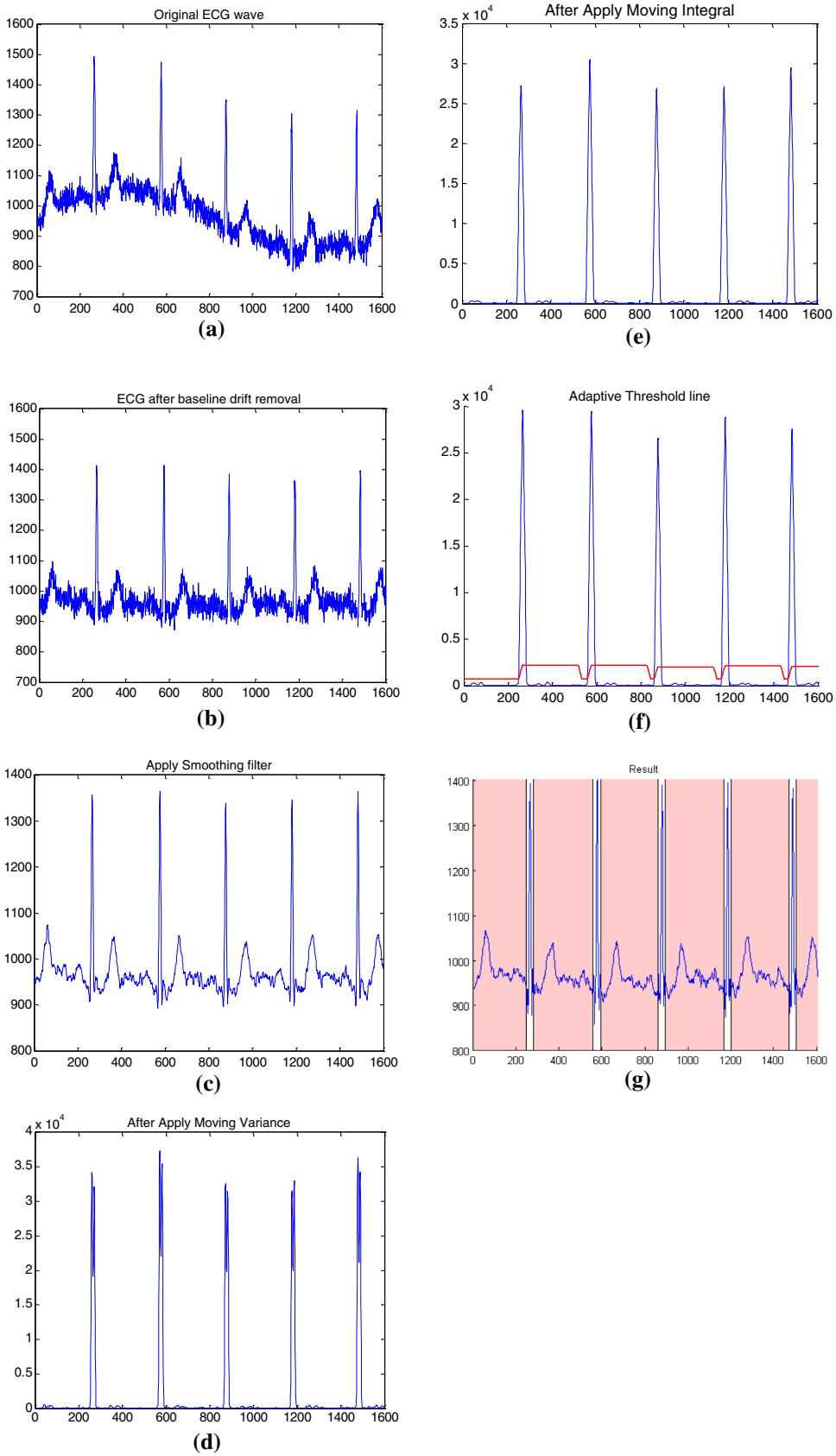

Fig. 7 ECG waveform transformation stages. **a** Original ECG wave with noise. **b** Step 1: ECG wave after baseline drift removal. **c** Step 2: ECG wave after smoothing filter. **d** Step 3: ECG wave after moving variance. **e** Step 4: ECG wave after moving integral. **f** Step 5: ECG wave after adaptive threshold. **g** Output ECG wave

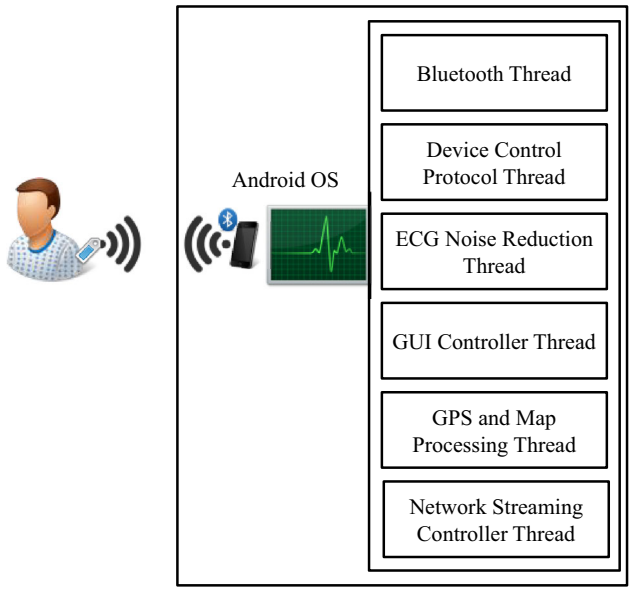

Fig. 8 Mobile ECG architecture

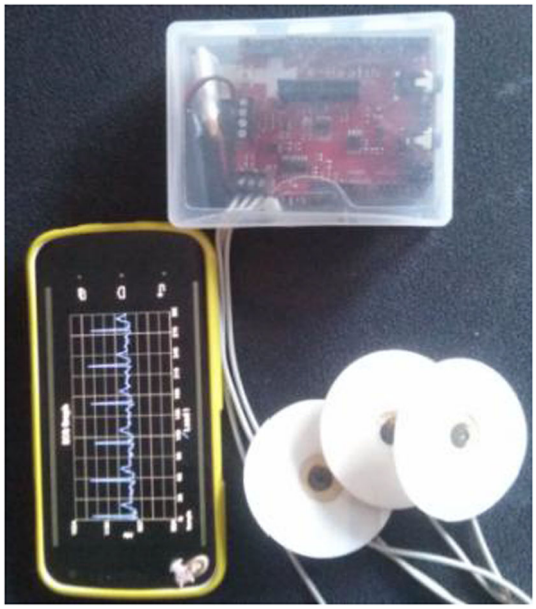

Fig. 10 Mobile ECG controller (prototype)

6.1 Experimental Set-up

For comparison purposes, the test bed was a standard configuration on a personal computer running the Windows 8 Ultimate operating system (64 bits): CPU Intel(R) Core(TM) i7-3632QM CPU @ 2.20GHz, 8192 MB DDR3-SDRAM, and 1 TB 7200 RPM Disk with MATLAB Toolbox [42]. We selected a Samsung Galaxy Nexus [5] as the mobile phone implementation platform because of its multi-functional features, which include Bluetooth interfaces with *e-health* sensor modules [41].

We were interested in evaluating two aspects of the method: noise reduction and QRS complex precision. For noise reduction, we intensively analysed the first sensor (lead) of the MIT-BIH arrhythmia database [43] over 109,809 beats. Three techniques were compared with the proposed system: simple moving average (SMA) [23], Savitzky–Golay [21], and PRASMMA [23]. Note that the Pan–Tompkins algorithm [29,44] does not include a noise reduction step.

Two metrics are typically used to evaluate the accuracy in the presence of noise, the signal-to-noise ratio (SNR), and root-mean-square deviation (RMSD). These are defined as [23]

$$\mathrm{SSNR} = \left(\frac{A_{\mathrm{filter}}}{A_{\mathrm{noise}}}\right)^2, \tag{9}$$

$$\mathrm{RMSD} = \sqrt{\frac{\sum_{i=1}^{n}\left(\mathrm{ECG}_{\mathrm{capture}}(i) - \mathrm{ECG}_{\mathrm{filter}}(i)\right)^2}{n}}. \tag{10}$$

As discussed in [23], it is hard to determine the validity of a raw ECG without a doctor's opinion. Thus, we added various types of noise [19] to a raw ECG wave ($\mathrm{ECG} + \mathrm{ECG}_{\mathrm{noise}} = \mathrm{ECG}_{\mathrm{capture}}$) and then measured the effectiveness of the algorithm by calculating the signal noise with smoothing ($\mathrm{ECG}_{\mathrm{filter}}$) and $\mathrm{ECG}_{\mathrm{capture}}$. When $\mathrm{ECG}_{\mathrm{filter}}$

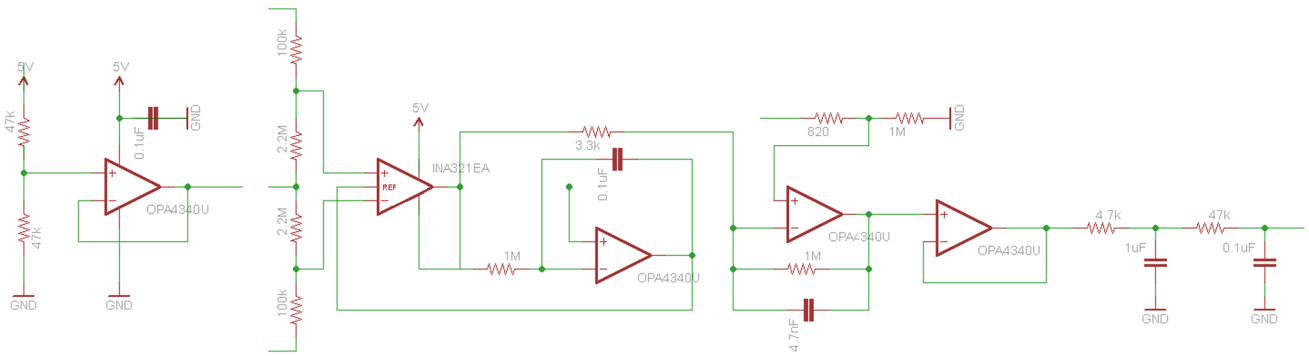

Fig. 9 *e-Health* sensor platform: schematic diagram [41]

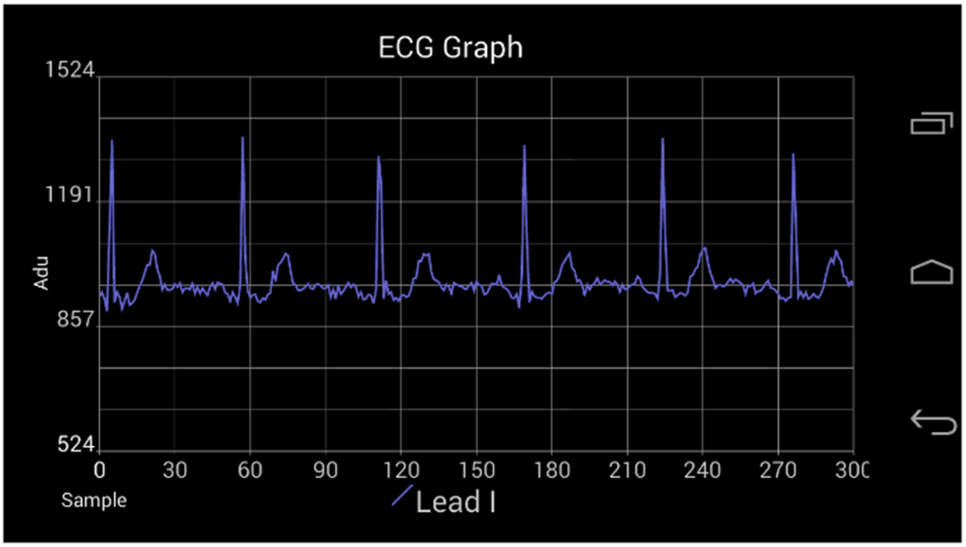

Fig. 11 Mobile phone screen interface: original waveform

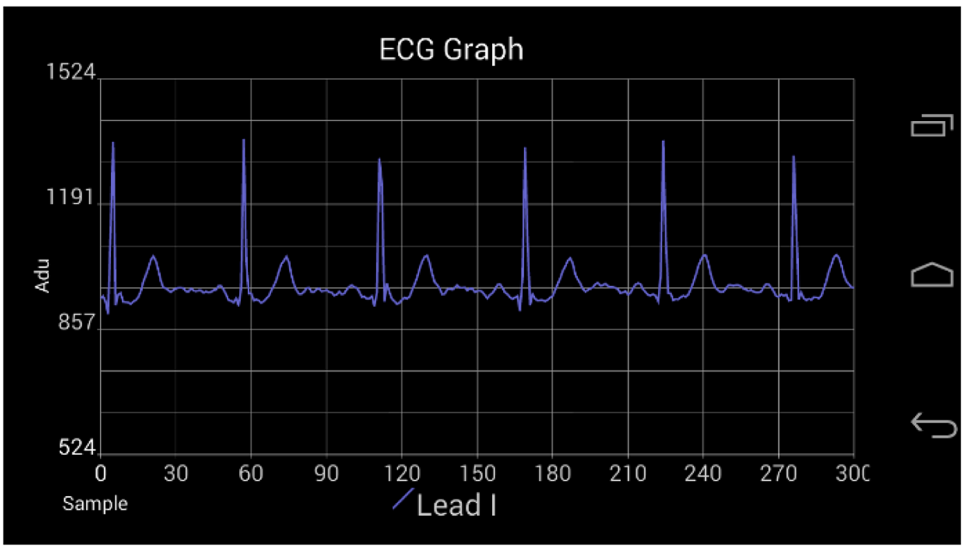

Fig. 12 Mobile phone screen interface: waveform after noise reduction

is close to ECG, the noise values should be close to the added noise, which leads to a similar RMSD.

The five noise types (power line [25], baseline wander, muscle (EMG) artefact, electrode motion artefact [24,27], and burst [19]) were combined (using *nstdbgen* tools [24,27]) and then varied by factors of 1 to 100. The SNR was used to measure the signal over the noise in terms of the amplitude (A).

We also acquired a raw ECG from a human subject to evaluate the real-time performance of the prototype. We recorded 2500 beats in two postures (sitting and standing), similar to [23]. Then, we used the peak SNR for our evaluations and comparisons. There is an assumption that the noise is already added in the ECG, and so this noise is approximately the remaining signal after applying the filter.

To investigate the accuracy of the detected QRS complex, we used a similar method to [45] for comparison purposes. We used a standard database for evaluating algorithms that measure QT and other waveform intervals in the ECG (the QTDB data set) [46] derived from records 100, 102, 103, 104, 116, 117, 123, 221, 223, 230, 231, 232, and 233 of the MIT-BIH arrhythmia database [43]. There were 1,100 QTDB beats in these records. Note that these records were verified by experts to determine the correct QRS complexes. We also added various noises, in the same way as the noise removal investigation.

We used three metrics to evaluate the feature extraction performance, $\mathrm{QRS}_{\mathrm{on}}$, $\mathrm{QRS}_{\mathrm{off}}$, and R_{peak}. We determined mean values and standard deviations. Values closer to zero represent a better precision than the database. Note that it is difficult to determine the exact QRS, or even its interval, as stated in [23]. So we only evaluated the PRASMMA, Pan–Tompkins, and RT-ECG methods using 1,100 samples from the QTDB database [24,43]. We selected the data set

Algorithm 1: Noise reduction with QRS complex detection
Input: current ECG samples (ecg_raw) from Bluetooth_buffer (i), f_s, and Q (sampling and cut-off frequencies)
Output: ECG_signal Y(i)

```
1. ecg_base(i)=a1×ecg_raw(i)+a2×ecg_raw (i-1)+a3×ecg_raw(i
   -2)-b1×ecg_base(i-1)-b2 × ecg_base(i-2)        //Step 1
2. for k=-(m-1)/2 to (m-1)/2                      //Step 2
3.          S(i) := C(k) × ecg_base(i);
4. end for
5. for j=0 to w                                   //Step 3
6.          Sbar(i) :=  Sbar(i) + S(i-j)/w;
7. end for
8. for j=0 to w
9.          V(i) = V(i) + (S(j) - Sbar(i))^2/w
10. end for
11. for j=0 to M-1                                //Step 4
12.         K(i) = K(i) + V(i-j)/M;
13. end for
14. A(i) = max(K(i-fs) × C1);                     //Step 5
15. if A(i) > A(i-1)  then
16.         T(i) = T(i-1) + (abs(A(i) - A(i-1)) × C2);
17. else if A(i) < A(i-1)         then
18.         T(i) = T(i-1) - (abs(A(i) - A(i-1)) × C2);
19.         end if
20. else   T(i) = T(i-1);
21. end if
22. if K(i) < T(i)     then       Y(i) = S(i);
23. else   Y(i) = ecg_base(i);
24. end if
```

from Table 2.A: records from MIT-BIH arrhythmia database, and Table 2.C: records from MIT-BIH supraventricular arrhythmia database excluding the first and final beat. The public baseline Pan–Tompkins implementation was provided by Sedghamiz [44].

We also recorded a number of R beats using the three algorithms, for 109,809 beats from the first MIT-BIH sensor with various added noise. At this stage, we used five metrics to evaluate the algorithms, that is, the total number of beats, false positive (FP), false negative (FN), failed detection, and accuracy [29], so that we could compare the performance to the results of Pan and Tompkins [29]. Moreover, we evaluated the same three algorithms against manually counted beats from the raw ECG from the human subject, for 2500 samples.

6.2 Experimental Results and Discussion

Figure 13 shows the SNR for various combined noises. The SNR generally reduced exponentially as the noise increased. The smallest difference between the signal after applying the filter and the typical wave (capture) represented the best performance (least error). Here, RT-ECG's SNR was the best, followed by Savitzky–Golay, PRASMMA, and SMA.

Figure 14 shows the RMSD for various noise levels. In general, the RMSD tended to increase with the noise. Similar to figure 13, RT-ECG' RMSDs are close to the typical wave which represented the best performance because RT-ECG preserved the QRS complex for the doctors' investigations,

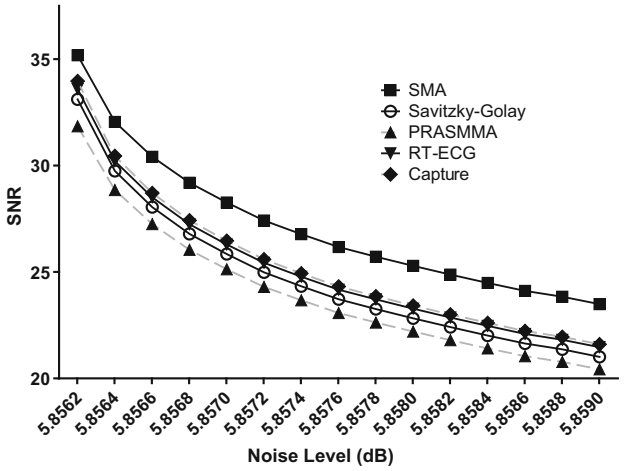

Fig. 13 Noise reduction performance: SNR for different noise levels

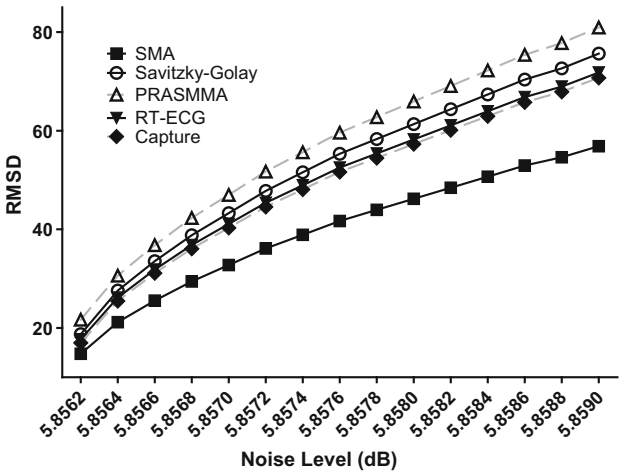

Fig. 14 Noise reduction performance: RMSD for different noise levels

followed by Savitzky-Golay, PRASMMA, and especially SMA which smoothes the QRS period.

Table 1 shows the noise reduction results for the raw human ECG during the two actions. RT-ECG had the smallest RMSDs (0.31 and 0.15) and the highest SNRs (19.97 and 25.72) and PSNRs (29.82 and 35.15). PRASMMA's SNR and PSNR are lower but higher for RMSD. The performance of Savitzky-Golay and SMA produced very similar results.

Table 2 shows the precision of the detected QRS complexes based on the QTDB data set with noise. RT-ECG generally outperformed PRASMMA (i.e. the means were closer to zero).

Table 3 compares the calculated number of R beats from the MIT-BIH data for various noise levels. RT-ECG generally performed best in terms of the FP, failed detection, and accuracy (99.98 %), compared with Pan–Tompkins (99.96 %), followed by PRASMMA (99.79 %). As stated in [29], potentially misleading results are associated with abnormal beats

Table 1 Noise reduction performance (raw human ECG) during two actions (sitting and standing), in terms of the RMSD, SNR, and PSNR

Algorithm	ECG test 1 (sit)			ECG test 2 (stand)		
	RMSD	SNR	PSNR	RMSD	SNR	PSNR
SMA	0.37	17.97	23.45	0.26	23.20	28.20
Savitzky–Golay	0.36	17.24	22.77	0.27	22.99	27.97
PRASMMA	0.36	19.12	24.65	0.18	27.51	32.58
RT-ECG	0.31	19.97	25.72	0.15	29.82	35.15

Table 2 Feature extraction results for the QTDB data set (RT-ECG, PRASMMA, and Pan–Tompkins)

Algorithm		QRS_{on}	R_{peak}	QRS_{off}
RT-ECG	# ann. beats	1100	1100	1100
	$\mu \pm \sigma$ (ms)	14.538± 13.98	−11.076±24.387	12.547±29.108
	σ (samples)	3	6	7
PRASMMA	# ann. beats	1100	1100	1100
	$\mu \pm \sigma$ (ms)	32.628±35.728	−11.946±44.411	−41.417±62.306
	σ (samples)	9	11	16
Pan–Tompkins	# ann. beats	1100	1100	1100
	$\mu \pm \sigma$(ms)	28.135±15.454	−14.206±21.735	−39.848±40.029
	σ (samples)	4	5	10

Table 3 Performance measurement (number of beats) for the MIT-BIH data (RT-ECG, PRASMMA, and Pan–Tompkins)

	FP (beat)	FN (beat)	Failed detection (beat)	Failed detection (%)	Accuracy (%)
RT-ECG	1986	370	2356	0.021455	99.97854
PRASMMA	12,737	10,775	23,512	0.214117	99.78588
Pan–Tompkins	2757	1956	4713	0.042920	99.95708

Table 4 Performance measurement (number of beats) for the raw human ECG (RT-ECG, PRASMMA, Pan–Tompkins, and manual beat count)

Algorithm	ECG test 1 (sitting) (beat)	ECG test 2 (standing) (beat)
RT-ECG	2780	2657
PRASMMA	2650	2546
Pan–Tompkins	2780 (2 beat skewed)	2657 (4 beat skewed)
Manual beat count	2780	2657

or different human behaviours. This can lead to faster or slower heart beat rhythms, if we only consider the static RR interval.

To illustrate the practical performance of this method, Table 4 shows the number of R beats based on the raw human ECG. The results are similar to those from MIT-BIH. The Pan–Tompkins and RT-ECG produced similar results and were superior to PRASMMA. However, the Pan–Tompkins prediction misinterpreted 2 and 4 beats (and PRASMMA misinterpreted 100 beats).

7 Conclusions and Future Work

We developed a novel, real-time, low-complexity ECG detection method with noise reduction. Our QRS complex detection procedure is called the RT-ECG. To adjust the baseline drift, we applied a bi-quad high-pass filter. Then, we used the moving window variance and integral with thresholds to detect the boundary of the QRS complex and applied the Savitzky–Golay smoothing filter. These steps are necessary for accurate medical diagnoses.

We compared the proposed method to other noise reduction and QRS complex detection techniques (SMA, Savitzky–Golay, PRASMMA, and Pan–Tompkins). RT-ECG performed the best when applied to the standard QT and MIT-BIH databases with added noise and to a raw ECG acquired from a human subject. RT-ECG generally outperformed the other techniques, producing more accurate results and preserving the QRS complex.

We implemented our method on a Samsung Galaxy Nexus Android OS mobile phone for practicality. However, although the proposed technique has significantly improved the performance, more investigations and analy-

ses are required. For example, we should examine various ECG patterns and abnormal behaviours.

Moreover, it may be possible to reduce noise caused by electronic parts such as ECG sensor tags. Finally, to illustrate the technique's practical medical use, equipment with certified biosafety standards should be investigated and compared with open-platform medical devices. This method shows great promise, although there are aspects that need further research.

Acknowledgments This research was supported in part by a research grant provided by Khon Kaen University, Thailand.

References

1. Cacti: The Atlas of heart disease and stroke cacti. [www.who.int] (2009)
2. Holden, R.J.; Karsh, B.T.: The technology acceptance model: its past and its future in health care. J. Biomed. Info. **43**(1), 159–172 (2010)
3. Wu, S.; Chaudhry, B.; Wang, J.; Maglione, M.; Mojica, W.; Roth, E.; Morton, S.C.; Shekelle, P.G.: Systematic review: impact of health information technology on quality, efficiency, and costs of medical care. Anal. Int. Med. **144**(10), 742–752 (2006). http://annals.org/article.aspx?articleid=723406
4. Cavallari, R.; Martelli, F.; Rosini, R.; Buratti, C.; Verdone, R.: A Survey on wireless body area networks: technologies and design challenges. IEEE Commun. Surv. Tutor. **99**, 1–23 (2014)
5. Samsung Galaxy Nexus. [www.samsung.com/us/mobile/cell-phones/GT-I9250TSGGEN] (2013)
6. Brian, R.M.; Ben-Zeev, D.: Mobile health (mHealth) for mental health in Asia: objectives, strategies, and limitations. Asian J. Psychiatry **10**, 96–100 (2014)
7. Busis, N.: Mobile phones to improve the practice of neurology. Neurol. Clin. **28**(2), 395–410 (2010)
8. So-In, C.; Phaudphut, C.; Rujirakul, K.; Phokaped, N.; Poolsanguan, S.; Waikham, B.: A novel architecture for mobile ECG recognition systems using hybrid wavelet transform feature extraction schemes. J. Converg. Info. Technol. **8**(11), 471–484 (2013)
9. So-In, C.; Arch-Int, S.; Phaudphut, C.; Rujirakul, K.; Weeramongkonlert, N.: A new mobile phone system architecture for navigational travelling blind. In: Proceedings of the International Joint Conference on Computer Science and Software Engineering. Thailand, pp. 54–59 (2012)
10. Al-Zaben, A.; Hamad, A.; Alfahoum, A.; Saefan, W.: Heart rate variability while listening to Quran recitation. Arab J. Sci. Eng. **39**(2), 1129–1133 (2014)
11. Clifford, G.D.; Azuaje, F.; McSharry, P.E.: Advanced Methods and Tools for ECG Data Analysis, pp. 384. Artech House Publishers, Boston (2006)
12. Dettori, L.; Semler, L.: A comparison of wavelet, ridgelet, and curvelet-based texture classification algorithms in computed tomography. Comput. Biol. Med. **37**(4), 486–498 (2007)
13. Adam, G.; Witold, P. (eds.): ECG Signal Processing, Classification and Interpretation, Biomedical Engineering. pp. 278 (2012)
14. Li, J.; Zhou, H.; Zuo, D.; Hou, K.M.; Vaul, C.D.: Ubiquitous health monitoring and real-time cardiac arrhythmia detection: a case study. Bio-Med. Mater. Eng. **24**(1), 1027–1033 (2014)
15. Tanantong, T.; Nantajeewarawat, E.; Thiemjarus, S.: Toward continuous ambulatory monitoring using a wearable and wireless ECG- recording system: a study on the effects of signal quality on arrhythmia detection. Bio-Med. Mater. Eng. **24**(1), 391–404 (2014)
16. Messaoud, M.B.; Khelil, B.; Kachouri, A.: Analysis and parameter extraction of P-wave using correlation method. Int. Arab J. Info. Technol. **6**(1), 40–46 (2009)
17. Akshay, N.; Jonnabhotla, N.A.V.; Sadam, N.; Yeddanapudi, N.D.: ECG Noise removal and QRS complex detection using UWT. In: Proceedings of the International Conference on Electronics and Information Engineering. Kyoto, Japan, pp. 438–442 (2010)
18. Boucheham, B.: Dimensionality reduction in time series: a PLA-block-sorting method. Int. Arab J. Info. Technol. **4**(4), 307–312 (2007)
19. Rabya, B.K.; Hoti, R.B.K.; Khattak, S.: Automated noise removal and feature extraction in ECGs. Arab J. Sci. Eng. **39**, 1937–1948 (2014)
20. Dliou, A.; Latif, R.; Laaboubi, M.; Maoulainine, F.M.R.: Abnormal ECG signals analysis using non-parametric time–frequency technique. Int. Arab J. Info. Technol. **39**(2), 913–921 (2014)
21. Luo, J.; Ying, K.; Bai, J.: Savitzky–Golay smoothing and differentiation filter for even number data. Signal Process. **85**, 1429–1434 (2005)
22. Savitzky, A.; Golay, M.: Smoothing and differentiation of data by simplified least squares procedures. Anal. Chem. **36**(8), 1627–1639 (1964)
23. Pandya, U.T.; Desai, U.B.: A novel algorithm for bluetooth ECG. IEEE Trans. Biomed. Eng. **59**(11), 3148–3154 (2012)
24. Moody, G.B.; Muldrow, W.E.; Mark, R.G.: A noise stress test for arrhythmia detectors. Comput. Cardiol. **11**, 381–384 (1984)
25. Levkov, C.; Mihov, G.; Ivanov, R.; Daskalov, I.; Christov, I.; Dotsinsky, I.: Removal of power-line interference from the ECG: a review of the subtraction procedure. BioMed. Eng. Online **4**(50), 1–18 (2005)
26. Lo, C.; Turner, D.D.; Knuteson, R.O.: A principal component analysis noise filter value-added procedure to remove uncorrelated noise from atmospheric emitted radiance interferometer (AERI) observations. Pacific Northwest National Laboratory, ARM TR-071, USA (2006)
27. Goldberger, A.L.; Amaral, L.A.; Glass, L.; Hausdorff, J.M.; Ivanov, P.C.; Mark, R.G.; Mietus, J.E.; Moody, G.B.; Peng, C.K.; Stanley, H.E.: "PhysioBank, physioToolkit, and physioNet: components of a new research resource for complex physiologic signals. Circulation **101**(23), e215–e220 (2000)
28. Castells, F.; Laguna, P.; Sornmo, L.; Bollmann, A.; Roig, J.M.: Principal component analysis in ECG signal processing. EURASIP J. Adv. Signal Process. (2007). http://asp.eurasipjournals.com/content/pdf/1687-6180-2007-074580.pdf4
29. Pan, J.; Tompkins, W.J.: A real-time QRS complex detection algorithm. IEEE Trans. Biomed. Eng. EME-32, no. 3 (1985)
30. Zeraatkar, E.; Kermani, S.; MehriDehnavi, A.; Aminzadeh, A.: Improving QRS complex detection for artifacts reduction. In: Proceedings of the International Conference on Biomedical Engineering. Isfahan, Iran, pp. 1–4 (2010)
31. Lina, Z.; Xinhua, J.: The pretreatment and feature data extraction of ECG based on matlab. In: Proceedings of the International Conference on Bioinformatics and Biomedical Engineering. Wuhan, China, pp. 1–4 (2011)
32. Lewandowski, J.; Arochena, H.E.; Naguib, R.N.G.; Chao, K.: A simple real-time QRS complex detection algorithm utilizing curve-length concept with combined adaptive threshold for electrocardiogram signal classification. In: Proceedings of the International Conference on TENCON. Cebu, Philippines, pp. 1–6 (2012)
33. Changmok, C.; Younho, K.; Kunsoo, S.: A PD control-based QRS complex detection algorithm for wearable ECG applications. In: Proceedings of the International Conference on Engineering in

Medicine and Biology Society. San Diego, USA, pp. 5638–5641 (2012)
34. Arafat, M.A.; Mahmud, T.B.; Billah, M.S.: Retrieving and smoothing fundamental waves from noise corrupted ECG beat using gaussian functions. In: Proceedings of the International Conference on Electrical and Computer Engineering. Dhaka, Bangladesh, pp. 153–156 (2012)
35. Perlman, O.; Katz, A.; Zigel, Y.: Noninvasive fetal QRS complex detection using a linear combination of abdomen ECG signal. In: Proceedings of the International Conference on Computing in Cardiology. Zaragoza, Spain, pp. 169–172 (2013)
36. Gradl, S.; Kugler, P.; Lohmuller, C.; Eskofier, B.: Real-time ECG monitoring and Arrhythmia detection using android-based mobile device. In: Proceedings of the International Conference on Engineering in Medicine and Biology Society. Zaragoza, Spain, pp. 2452–2455 (2012)
37. Chan, C.C.; Chieh, C.W.; Wei, C.C.; Lwun, H.Y.; Hung, L.Y.; Pin, M.H.: Energy efficient diagnostic grade mobile ECG monitoring. In: Proceedings of the International Conference on New Circuits and Systems. Montreal, Canada, pp. 153–156 (2012)
38. Kuo, S.M.; Lee, B.H.; Tian, W.: Real-Time Digital Signal Processing: Fundamentals, Implementations and Application, pp. 564. Wiley, London (2013)
39. Manpreet, K.; Birmohan, S.; Seema.: Comparisons of different approaches for removal of baseline wander from ECG signal. In: Proceedings of the International Conference on Emerging Trends in Technology. New York, USA, pp. 30–36 (2011). http://ijcaonline.org/proceedings/icwet/number5/2099-bm254
40. The Android framework APIs. [developer.android.com/guide/topics/graphics/2d-graphics.html] [developer.android.com/guide/topics/connectivity/bluetooth.html] (2014)
41. ehealth-sensors-complete-kit-biometric-medical-arduino-raspberry-pi, [www.cooking-hacks.com/ehealth-sensors-complete-kit-biometric-medical-arduino-raspberry-pi] (2014)
42. Matlab Toolbox. [www.matlab.com] (2014)
43. Moody, G.B.; Mark, R.G.: The MIT-BIH arrhythmia database. Comput. Cardiol. [ecg.mit.edu](1990)
44. Sedghamiz, H.: Complete Implementation of Pan-Pan-Tompkins Algorithm. Linkoping University. [www.mathworks.com/matlabcentral/fileexchange/45840-complete-pan-Pan-Tompkins-implementation-ecg-qrs-detector] (2014)
45. Mazomenos, E.B.; Biswas, D.; Acharyya, A.; Chen, T.; Maharatna, K.; Rosengarten, J.; Morgan, J.; Curzen, N.: A low-complexity ECG feature extraction algorithm for mobile healthcare applications. IEEE J. Biomed. Health Info. **17**(2), 459–469 (2013)
46. Laguna, P.; Mark, R.G.; Goldberger, A.L.; Moody, G.B.: A database for evaluation of algorithms for measurement of QT and Other waveform intervals in the ECG. Comput. Cardiol. **24**, 673–676 (1997)